Proceedings World Geothermal Congress 2015
Melbourne, Australia, 19-25 April 2015

Thermal Performance of the Cerro Prieto Geothermal Field Fluid Transportation Network

Alfonso Garcia-Gutierrez[1], Juan. I. Martinez-Estrella[1], Rosember Ovando-Castelar[1], Ismael Canchola-Félix[2], Paul Jacobo-Galvan[2]

[1]Instituto de Investigaciones Eléctricas, Ave. Reforma 113, Palmira, Cuernavaca, Mor., 62490 México

[2]Comisión Federal de Electricidad, Residencia Cerro Prieto, Km.25 Carr. Mexicali-Pascualitos-Pescaderos, B.C., México

aggarcia@iie.org.mx

Keywords: Cerro Prieto, transportation network, thermal performance, first and second law efficiency, heat and mass losses.

ABSTRACT

The thermal performance at the Cerro Prieto Geothermal Field (CPGF) fluid transportation network was evaluated in terms of the mass, energy and exergy flows of the separated steam and water at selected points of the transportation network, the mass and heat losses from the separators, pipelines and fittings, and the partial (transportation sub-processes) and overall (wellhead to power plant inlet) thermal efficiencies. Thermal efficiencies of the transportation sub-processes and overall steam field (wellhead to power plant inlet) processes were also evaluated. The 1st law efficiencies range from 86.8 to 98.1% for the individual fluid transportation sub-processes while those of the 2nd law vary from 78.9 to 95.9%. The overall efficiencies are 67.6% and 75.2 %, respectively. Total heat losses from the HP and LP gathering networks amounted to 180.6 MWt of which 72.9 MWt were lost through the pipelines thermal insulation, 33.7 MWt from the pipelines fittings, and 74.0 MWt from the condensate drains. Potential areas for improvement of energy utilization were detected and evaluated, and showed a potential for energy recovery equivalent to 83 MWe of additional capacity while maintaining the same rate of fluid and energy extraction and the same number of producing wells.

1. INTRODUCTION

In geothermal fields, the fluid from producing wells is usually transported through a network of pipelines to the power plants which may be sited several hundred of meters or even some kilometers away. Thus, the performance of the pipeline transportation network is affected among others, by the type of fluid being transported (one- or two-phase), the network geometry and complexity, the actual thermal insulation condition and steam field operating strategies. In fact, one of the largest problems in analyzing pipeline network behavior is the difficulty in accounting for the actual component operational and physical features as some conditions change from the design specifications. This occurs, for example, when the pipelines thermal insulation deteriorates with time, or when pipelines carry less fluid than the flow specified at normal operation conditions, etc. Hence, the departure from operational design specifications of the pipeline network components and operating philosophy are some of the factors that affect the fluid transportation network thermal performance.

Energy-exergy analysis of geothermal fields started with the Larderello six-well network evaluation by Marconcini and Neri (1979). Further analysis of other geothermal fields appeared subsequently (Betaggli and Bidini, 1996; DiMaria, 2000; White and Morris, 2000; Quijano, 2000; Kwambai, 2005; Kaplan and Schochet, 2005; Aqui et al., 2005; Otzurk et al., 2006). Regarding Mexican geothermal fields, Garcia-Gutierrez et al. (2012, 2013) performed an analysis for improving energy utilization in the CPGF and evaluated the thermal performance of the Los Humeros Geothermal Field (LHGF), respectively. Heat transfer in the CPGF gathering system was analyzed by Peña (1986) and Peña and Campbell (1988) who determined the energy losses in a horizontal large diameter, thermally insulated pipe network. However, the examples shown include relatively short pipes and a small number of wells when compared to the actual CPGF total system. Ovando-Castelar et al. (2012) estimated the heat losses at the CPGF gathering system considering the physical condition of the pipeline thermal insulation. Other models (Schroeder, 1982; Marconcini and Neri (1979) showed calculation methodologies of the temperature at the surface of thermal insulations and the heat gains or losses through a tube, while varying other factors. These models include conduction, convection and radiation for heat loss calculation in thermally insulated pipes.

This paper describes an energy analysis of the CPGF fluid transportation system to evaluate its thermal performance, the source of main energy losses and a summary of the evaluation of several areas of opportunity with potential for improving utilization. The study is a snapshot of the plant´s operation on June 2009 and covers only the fluid production and transportation system, and excludes the existing power plants.

2 DESCRIPTION OF THE CPGF STEAM GATHERING NETWORK

The Cerro Prieto geothermal field is the largest liquid-dominated geothermal field in the world with an installed capacity of 720 MWe and thirteen condensing power plants however the currently operating capacity is 570 MWe. The field comprises four areas named Cerro Prieto-1 (CPU), Cerro Prieto-2 (CPD), Cerro Prieto-3 (CPT) and Cerro Prieto-4 (CPC). Separated steam from 165 producing wells feeds the power plants through a complex gathering system that includes HP and LP networks. The networks have lengths of 92.1 km and 47.6 km, respectively, totaling 139.6 km. Pipeline diameters range from 8” to 48” and were originally insulated with a 2” layer of mineral wool or glass fiber, and an exterior metallic cover of aluminum or wrought iron.

Steam is separated at each production well and individual pipelines transport it to the sub-or main-collectors. The network is highly complex and has several arrangements for steam separation. CPU has HP steam separation only, whereas CPD, CPT and CPC have both HP and LP separation. In CPD and CPT there are several “sites” for steam separation. In a “site”, the HP steam is separated first and the separated water is sent to the LP separator together with the brine from other neighboring wells. In CPC there are “separation islands”, which are square areas, divided into four modules. Each module has four HP separators that receive the two-phase flow from four wells to separate HP steam. Then, the separated water of the four streams is mixed and fed to a single

separator to obtain LP steam. There also exist some auxiliary wells, which do not actually produce water or steam, but their facilities are used to separate the steam from the fluid produced by a neighbor well.

CPU has eight HP branches while CPD, CPT and CPC have both HP and LP parallel branches, two per field area. The steam transportation network also has several interconnections among the different field areas to ensure an adequate steam supply to the power plants. The large majority of the separated water is finally sent to an evaporative pond via open channels, however some of the separated water is injected either hot or cold. Fig. 1 shows the steam gathering network of the entire geothermal field.

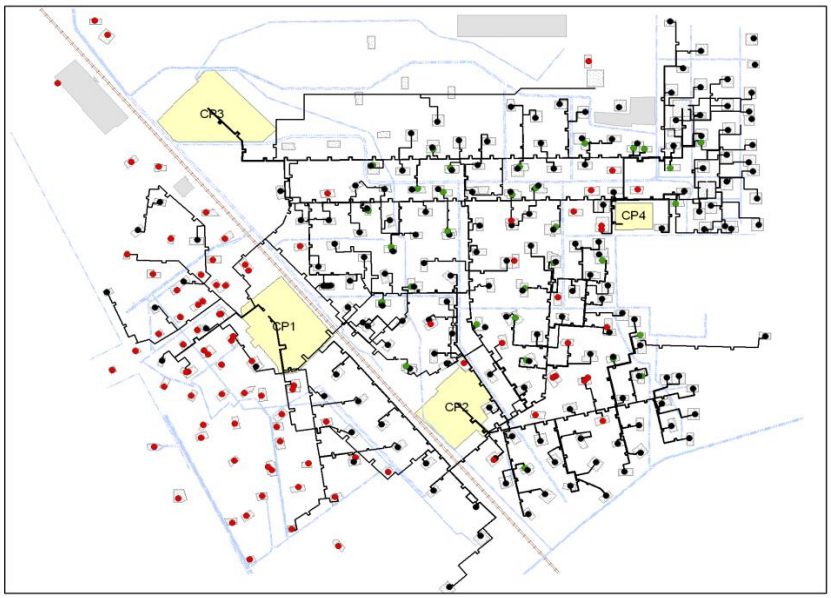

Figure 1. The Cerro Prieto geothermal field steam transportation network.

3. METHODOLOGY

3.1 Energy and exergy

Energy and exergy are defined (DiPippo, 2005) as

$$e_n = \dot{m}\, h \tag{1}$$

$$e_x = \dot{m}\left[\left(h_i - h_o\right) - T_o\left(s_i - s_o\right)\right] \tag{2}$$

where e_n denotes energy, e_x is exergy, h enthalpy, $\dot{m}$ mass flow rate, s entropy and T temperature, the index 0 denotes the reference state or ambient conditions and index i indicates the system conditions at point i.

Energy and exergy efficiencies are given by:

$$\eta_{e_n} = e_{n_{out}} / e_{n_{in}} \tag{3}$$

$$\eta_{e_x} = e_{x_{out}} / e_{x_{in}} \tag{4}$$

where η denotes efficiency and the indexes in and out denote inlet and outlet.

3.2 Heat losses from pipelines

Heat losses from the pipelines Q were computed according to the physical condition of the insulation materials using Eq. (5). Insulation surface temperatures were measured for this purpose.

$$Q = U\ A\ \Delta T \tag{5}$$

where U is the overall heat transfer coefficient; A is the surface area and ΔT is the temperature difference between the surface of the thermal insulation material and the ambient.

U depends on the length and diameter of each pipe length and on the physical condition of the insulating materials. Since some of the insulations presented wear, geometric deformation, loss of outer cover, replacement of insulation type, or no insulation at all, an inventory was carried out to obtain actual information on the physical condition of the insulation materials throughout the gathering system. For this end, the insulation conditions were classified in four types or quality levels, coded with a letter and a color for each condition, according to their physical conditions as shown in Fig. 2.

Physical condition of insulation	Key	Color
New or complete	A	
Good but no metallic cover	B	
Regular or deteriorated	C	
Absent, totally destroyed	D	

Figure 2. Classification of the CPGF gathering network insulation materials physical condition.

3.3 Heat losses from fittings

Heat losses from the pipeline fittings were computed from their geometrical information and measured surface temperatures. Since practically all fittings were uninsulated, calculations were carried considering that a portion of the fitting surface area (base area) losses heat by convection and radiation in a similar way as a bare pipe does, and that the rest of the surface area (secondary area) behaves like a fin dissipating heat by convection and radiation with a given efficiency. Heat loss from fittings Q_f are defined as:

$$Q_f = UA_b \Delta T + \eta_f A_f \Delta T \tag{6}$$

where U is the overall heat transfer coefficient for convection and radiation, A_b and A_f are the fitting base and secondary surfaces areas, and η_f is the fin efficiency. For fins of rectangular cross section η_f is given (Incropera et al., 2006) by:

$$\eta_f = \frac{\tanh(m L_c)}{m L_c} \tag{7}$$

and where m = $(2w/kt)^{1/2}$ and Lc = L + (t/2). In these equations, L, w, t and k are the length, width, thickness and thermal conductivity of the fin, respectively.

3.4 Heat losses from condensate drains

Energy losses from condensate drains were obtained by subtracting the heat losses from the pipelines and fittings from the total energy losses occurring in the HP and LP gathering networks. The total energy losses were computed from operational data at the inlet and outlet of both networks.

$$Q_d = Q_{net} - (Q_p + Q_f) \tag{8}$$

where Q_d are the heat losses from the condensate drains and Q_{net} are the total energy losses occurring in either the HP or LP gathering networks.

4. RESULTS

4.1 Performance of the CPGF gathering network

In order to evaluate the CPGF transportation network performance, mass, energy and exergy flows were computed from Eqs. (1) and (2) using operative and environmental data of June 2009. These flows were evaluated at three boundaries: F1 (wellhead), F2 (the outlet of steam and water from the HP and LP separators), and F3 (the power plant steam delivery points). Then, partial and overall efficiencies were computed using Eqs. (3) and (4). Fig. 3 shows schematically these boundaries and the corresponding mass, energy and exergy flows while Fig. 4 shows the 1st and 2nd law efficiencies of the partial and overall processes.

Fig. 3 shows that the HP steam after separation carries 63.5 and 74.0 % of the produced energy and exergy, respectively, whereas the low pressure steam after separation carries 7.5 and 7.3% of the produced energy and exergy, respectively. Also, about 61% of the produced fluid is liquid water, and carries about 27% of the thermal energy produced and about 14.5% of the exergy produced. Energy losses in the HP and LP networks amounted to 126 MWt and 54MWt, respectively, totaling 180.6 MWt. The corresponding exergy losses were 63, 21 and 84MWt. Energy losses from the separation process amount to 106 MWt or 2%.

Fig.4 shows that the separation process (boundaries B1and B2) had energy and exergy efficiencies of 98.1and 95.9%, respectively, whereas the overall transportation process (boundaries B1 and B3) had energy and exergy efficiencies of 67.6 and 75.2 %, respectively. The corresponding individual efficiencies are 96.3 and 93.7% for the HP network and 86.8 and 78.9% for the LP network (boundaries B2 and B3).

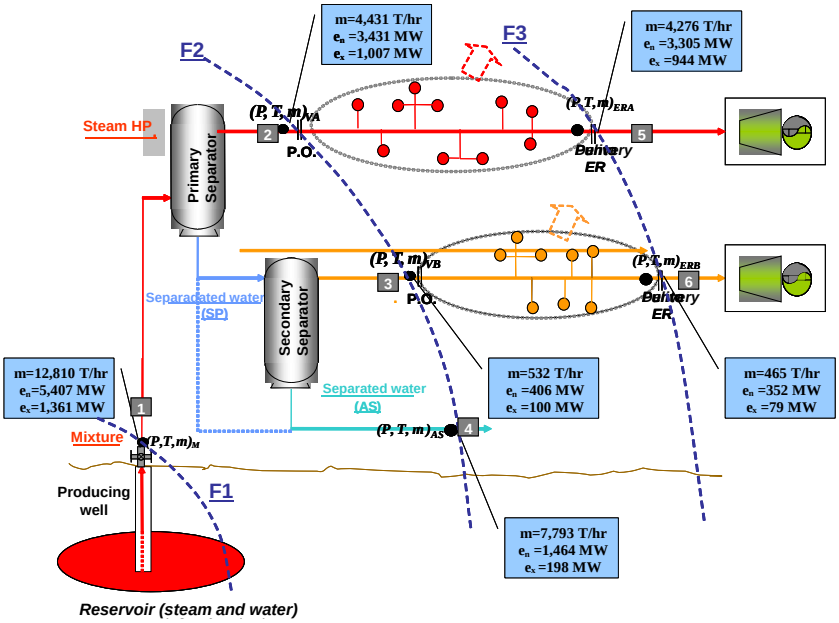

Figure 3. Mass, energy and exergy flows of the CPGF gathering system.

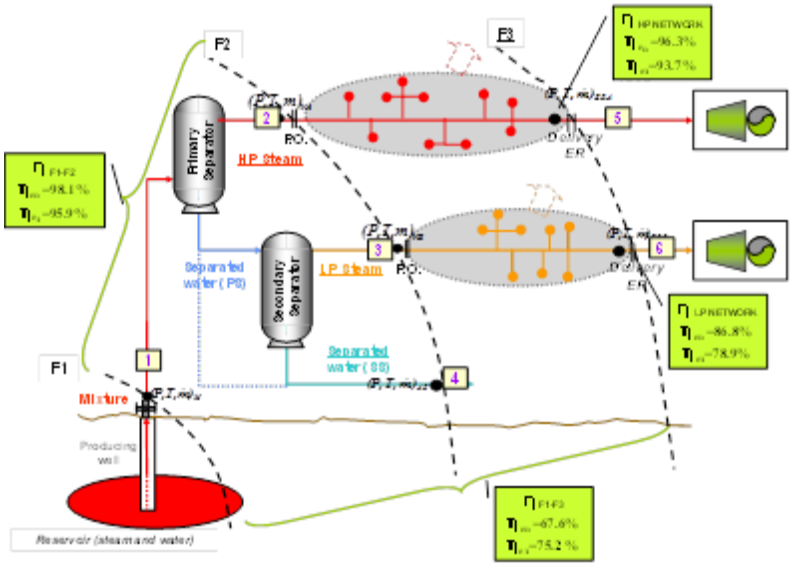

Figure 4. 1st Law (energy) and 2nd law (exergy) efficiencies of the CPGF gathering system.

4.2 Heat losses from pipelines

The data of the four types or quality levels of insulations conditions (described in Fig. 2) were compiled on hard-copy maps and fed to an MS Excel worksheet database, together with pipe diameter data. Subsequently, the information was transferred into a Geographical Information System (GIS) software package to create maps which helped to easily identify those parts of the gathering network where heat losses were higher and facilitated precise quantification of pipeline lengths corresponding to each insulation condition. Pipe diameters maps were also created. The procedure was applied to both the HP and LP gathering networks. Fig. 5 shows the map of the thermal insulations physical conditions of the HP gathering network.

According to the inventory, the total length of the operating steam pipeline transportation network is 139.7 km. From this total, 92.1 km (66%) correspond to the HP network and 47.6 km (34%) belong to the LP network. For both networks, about 80-82% of its total length has thermal insulations corresponding to qualities A and B which denote good condition, while the remaining 18-20% had insulations with qualities C and D (regular to very bad condition).

Once the length, diameter, insulation physical condition and operating conditions were collected, the overall heat transfer coefficients were computed for each insulation condition. The determination of this parameter constituted an extremely complex task, given the great variety of pipe diameters, different operating conditions, and different types and physical condition of the insulations in the pipe network. Calculations of the U´s were conducted by grouping the CPGF in two separate sectors, Cerro

Prieto-1 (CPU) and Cerro Prieto-2, 3 and 4 areas (CPDTC). The CPU sector has only HP steam lines however they operate at lower pressures and flow rates compared with CPDTC. For the CPDTC grouping, the calculations were carried out separately for the HP and LP networks. These calculations for insulation conditions or qualities A, B and D were performed by varying mass flow rate and pressure.

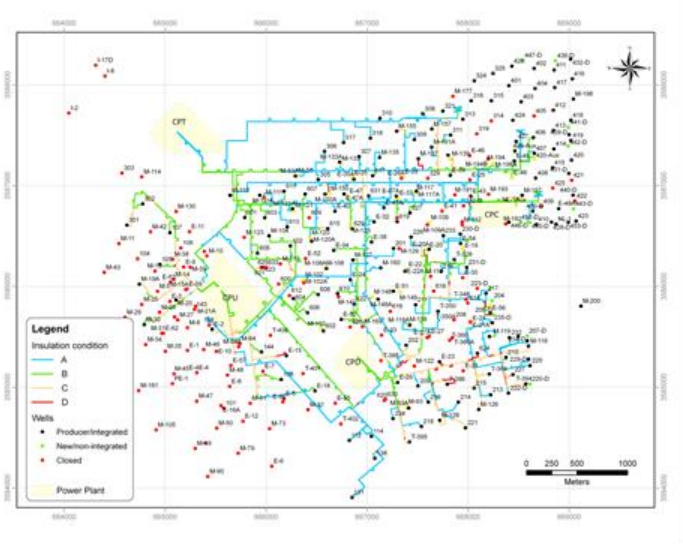

Figure 5. Map of the thermal insulations of the CPGF HP pipe network.

For condition C (regular or deteriorated), the calculations of heat loss were even more complicated due to the obvious loss of the cylindrical geometry due to irregular and reduced thickness and loss of portions of insulation. Surface temperature was defined as a benchmark for the heat loss. The surface temperature was obtained from averaging the field measured temperatures using two infrared thermo-graphic cameras and a laser infrared thermometer. Subsequently, through simulations performed with an MS Excel-based application program, the insulation thickness of each pipeline was reduced until the theoretical surface temperature fitted the average field-measured temperature. In this way, the reduction of the original insulation thickness related to the current physical condition was estimated to be 50% on the average (Ovando-Castelar et al., 2012). Table 1 shows the total heat losses of the CPDTC HP networks as function of their insulation condition and diameter. Similar results were obtained for the CPU and CPDTC LP networks.

Table 1. Total heat losses in the CPDTC HP steam gathering network.

Pipeline type	Nominal diameter [in]	Pipe Length [m]	Length A [m]	Length B [m]	Length C [m]	Length D [m]	Condition A [kWt]	Condition B [kWt]	Condition C [kWt]	Condition D [kWt]	Heat loss [kWt]
Single-well	14.00	1549.34	370.82	0.00	905.49	273.03	79.37	0.00	353.41	1052.70	**1485.47**
	16.00	5689.23	1333.12	1824.25	2079.90	451.97	326.55	453.62	935.32	1998.84	**3714.32**
	18.00	3459.79	990.57	1745.41	675.31	48.50	264.92	474.28	332.41	222.21	**1293.82**
	20.00	18851.48	12547.73	3856.78	1697.74	749.23	3711.44	1160.07	927.91	3757.97	**9557.39**
	22.00	306.67	0.00	0.00	306.67	0.00	0.00	0.00	175.11	0.00	**175.11**
	24.00	322.92	320.92	0.00	0.00	2.00	122.11	0.00	0.00	11.26	**133.36**
	SubTotal	**30179.43**	**15563.16**	**7426.44**	**5665.10**	**1524.73**	**4504.39**	**2087.97**	**2724.16**	**7042.97**	**16359.48**
Sub-collector	14.00	244.54	0.00	244.54	0.00	0.00	0.00	53.49	0.00	0.00	**53.49**
	18.00	0.00	0.00	0.00	0.00	0.00	0.00	0.00	0.00	0.00	**0.00**
	20.00	1972.23	908.30	562.66	501.27	0.00	269.69	169.90	276.27	0.00	**715.87**
	22.00	531.76	0.00	518.85	0.91	12.00	0.00	169.60	0.55	70.85	**240.99**
	24.00	1388.18	442.49	378.84	549.85	17.01	169.18	148.08	390.94	108.80	**817.00**
	28.00	877.08	225.94	462.70	188.43	0.00	98.97	207.54	154.23	0.00	**460.74**
	30.00	2111.73	2098.92	12.81	0.00	0.00	977.43	6.11	0.00	0.00	**983.54**
	32.00	214.93	116.80	97.54	0.59	0.00	57.61	49.33	0.54	0.00	**107.48**
	36.00	785.65	0.00	785.65	0.00	0.00	0.00	441.69	0.00	0.00	**441.69**
	SubTotal	**8126.09**	**3792.46**	**3063.58**	**1241.05**	**29.01**	**1572.88**	**1245.74**	**822.53**	**179.64**	**3820.80**
Main collector or branch	18.00	604.24	53.51	542.72	0.00	8.00	14.52	149.65	0.00	41.20	**205.36**
	22.00	329.13	0.00	284.41	0.00	44.72	0.00	93.58	0.00	269.79	**363.37**
	24.00	941.87	159.68	512.35	188.40	81.44	60.89	199.73	133.66	525.40	**919.68**
	26.00	173.40	0.00	164.94	0.00	8.46	0.00	68.91	0.00	58.06	**126.97**
	28.00	2914.24	23.79	2323.34	476.79	90.32	10.35	1035.16	387.84	655.56	**2088.92**
	30.00	24.67	24.67	0.00	0.00	0.00	11.39	0.00	0.00	0.00	**11.39**
	32.00	0.00	0.00	0.00	0.00	0.00	0.00	0.00	0.00	0.00	**0.00**
	34.00	252.22	0.00	157.89	93.75	0.59	0.00	83.20	90.46	4.93	**178.60**
	36.00	14093.62	7669.79	5364.81	876.19	182.83	4135.02	2969.82	888.75	1596.63	**9590.21**
	38.00	1092.18	0.00	247.67	526.35	318.16	0.00	143.62	559.59	2888.49	**3591.69**
	40.00	4302.01	4110.24	164.24	17.97	9.57	2422.56	99.51	19.97	90.07	**2632.11**
	42.00	7588.06	7342.49	47.06	198.50	0.00	4508.94	29.72	230.07	0.00	**4768.74**
	44.00	1035.32	713.75	72.62	248.94	0.00	455.72	47.72	300.24	0.00	**803.68**
	46.00	7381.70	3648.47	3577.89	120.56	34.77	2417.40	2440.75	151.00	360.22	**5369.38**
	48.00	562.83	534.81	0.00	0.00	28.02	367.08	0.00	0.00	298.54	**665.62**
	SubTotal	**41295.49**	**24281.21**	**13459.95**	**2747.45**	**806.89**	**14403.87**	**7361.38**	**2761.59**	**6788.88**	**31315.71**
	TOTAL	**79601.01**	**43636.82**	**23949.96**	**9653.60**	**2360.62**	**20481.14**	**10695.09**	**6308.27**	**14011.50**	**51496.00**

Table 2 shows the length, heat losses, equivalent steam condensation rate and power loss of the individual gathering networks.

Table 2. Estimated total heat losses, steam condensation rate and power loss in the CPGF steam gathering network.

Field area	Length [m]	%	q [MW_t]	m [t/h]	q [MW_e]
Total CPU	12477.9	8.9	6.4	11.5	1.2
Total CPDTC-HP	79601.0	57.0	51.5	99.4	13.1
Total CPDTC-LP	47622.7	34.1	15.0	25.4	3.3
TOTAL CP	**139701.6**	**100.00**	**72.9**	**136.3**	**17.6**

Comparison of these results with the total energy losses occurring in the steam gathering system, which amounted to 180.6 MWt (Fig. 3), (126.6 MWt and 54.0 MWt, for the HP and LP networks, respectively), indicates that the heat losses due to the current condition of the insulations represent approximately 46% and 28% of the total energy losses in the HP and LP networks, respectively. Furthermore, from the field insulation condition inventory, only 18-20% of the total pipeline network length had insulations with regular to very bad condition (qualities C and D, respectively). However, these pipelines account for nearly half of the heat losses, 48% and 43%, for the HP and LP pipeline networks, respectively.

4.3 Heat losses from fittings

Heat loss calculation from fittings was also a complex task due to their large number (hundreds or thousands), variety (valves, flanges, pipe legs, etc.), geometrical complexity (variety of types, sizes, designs) and operational conditions (high, medium and low pressure and flow magnitude). Heat loss calculations assumed that the fittings surface temperature is the saturation temperature corresponding to the operational pressure; the thermal conductivity of the fitting was the same as the pipe material and the ambient temperature is the average ambient temperature of the previous year. Using Eq. (6), the typical results for the various fittings are shown in Table 3.

Table 3. Typical heat losses from various fittings of the CPGF gathering network.

Fitting	Diameter	Class	r_1 [m]	r_2 [m]	t [m]	p [barg]	Tsat [°C]	k [W/(m²-°C)]	U [W/(m²-°C)]	Ta [°C]	η [%]	A_f [m²]	A_d [m²]	Q [Wt]
Flange	10	300	0.137	0.222	0.048	3.935	151.4	49.603	18.101	23.8	92.462	0.475	0.429	2005.546
Flange	10	900	0.137	0.273	0.070	3.935	151.4	49.603	18.101	23.8	86.839	0.901	0.429	2797.867
Blind Flange	40	300	0.508	0.619	0.114	11.348	189.3	48.395	17.821	23.8	93.507	2.419	1.609	11417.540
Butterfly Valve	20	300	0.254	0.387	0.064	4.494	155.5	49.665	15.020	23.8	90.114	1.280	1.164	4583.922
Sphere valve	36	300	0.457	0.635	0.111	4.017	152.1	50.800	7.417	23.8	94.500	2.860	0.243	2802.918
Register-man	24	300	0.305	0.457	0.070	4.017	152.1	50.257	11.119	23.8	91.483	1.750	0.875	3531.679
Fitting	**Pipe diameter**	**L [m]**	**w [m]**	**t [m]**	**L_c [m]**	**m**	**p [barg]**	**Tsat [°C]**	**k [W/(m²-°C)]**	**U [W/(m²-°C)]**	**Ta [°C]**	**η [%]**	**A_f [m²]**	**Q [Wt]**
Pipe leg or support	16	0.052	0.700	0.010	0.057	8.182	6.895	169.9	49.325	16.361	23.8	93.330	0.081	180.579

Table 4 shows the total heat losses from the CPGF fittings and pipeline legs or supports, expressed in energy (MWt), equivalent steam condensation and loss of equivalent electrical power.

Table 4. Total heat losses from the CPGF gathering network fittings and pipeline legs.

Field area	Fitings			Pipe legs or supports		
	Q [MWt]	m [t/h]	P [Mwe]	Q [MWt]	m [t/h]	P [Mwe]
Total CPU	0.38	0.66	0.07	2.74	4.69	0.62
Total CPDTC- HP	4.91	9.02	1.19	16.66	29.03	3.82
Total CPDTC- LP	0.93	1.58	0.21	7.71	13-13	1.73
Total CPGF	6.21	11.26	1.46	27.1	46.86	6.17

Total heat losses from all fittings and networks were found to be 33.3 MWt. Since total energy losses from the HP and LP gathering networks are 126.6 and 54.0 MWt, respectively (Fig.3), the corresponding combined heat losses of pipeline fittings and legs amount to 19.5 and 16.0 %. These combined heat losses and steam condensation translate into a loss of 7.63 MWe or 1.1% of the total installed capacity.

For validation purpose, a comparison of computed surface temperatures and heat losses from fittings and results obtained by modeling the fittings was carried out. Fig. 6 shows the model and results of modeling a 10", Class 300 Flange. Heat losses from the model were 1,763.3W while the estimated heat loss using the MS Excel spreadsheet were 1,785.3 W, or a 1.2% difference. Maximum model temperature was 155°C (pipe-flange contact) while saturation temperature was 154.2°C.

4.4 Heat losses from condensate drains

Using the results of sections 4.1 through 4.3 and Eq. (8), the total heat losses from condensate drains amounted to 73.8 MWt. Of these, 44.0 MWt correspond to the HP gathering network and 29.4 MWt to the LP network.

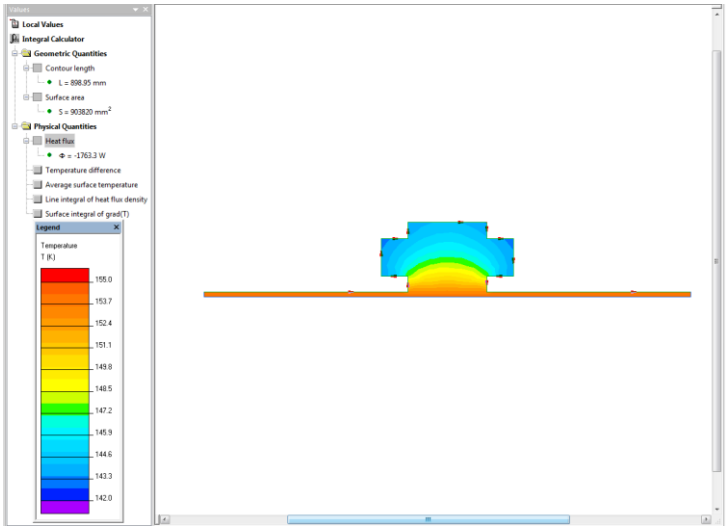

Figure 6. Model and results of a 10", Class 300 flange.

4.5 Summary of heat losses

Table 5 shows the total heat losses due to steam transport in the high- and low-pressure networks of the CPGF and a breakdown of the losses from pipeline insulations, fittings, supports and condensate drains.

Table 5. Heat losses of the HP and LP steam gathering networks and contributions by pipeline thermal insulations, pipeline fittings and legs, and condensate drains.

Gathering network	Energy losses due to transport [MWt]	Heat losses from pipeline insulation [MWt]	Heat losses from fittings and legs [MWt]	Heat losses from drains [MWt]
High-P	126.6	57.9	24.7	44.0
Low-P	53.5	15.0	8.6	29.8
TOTAL	180.1	72.9	33.3	73.8

4.6 Energy balance of the CPGF

Fig. 7 shows the overall heat balance of the CPGF showing the total energy produced by all wells, the heat loss due to steam separation, the heat carried out by the HP and LP steam, gathering system heat losses and energy delivered to the power plants. The figure also includes the heat balance of the separated water and its final disposal. It is easy to see that the separation and transportation processes offer areas of opportunity for improving energy utilization by reducing heat losses and steam condensation.

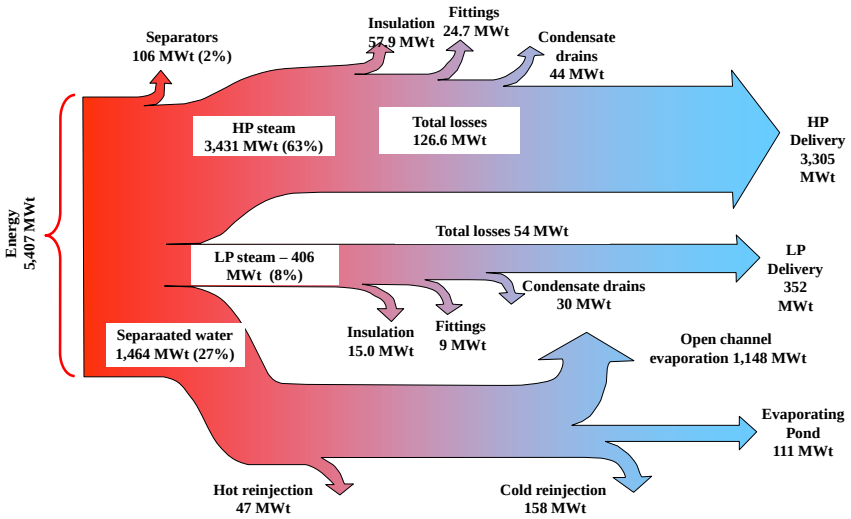

Figure 7. Overall energy balance of the produced fluids at the CPGF.

4.7 Potential for energy utilization improvement

From the present study, several areas of opportunity for energy recovery were detected and evaluated. The details of that study are given in a companion paper (Garcia-Gutierrez et al., 2015). Table 6 gives a summary of the cases that were analyzed. As seen form this table, the total potential for energy recovery in the CPGF is 83 MWe o which 72 MWe correspond to the potential of additional power generation within the steam field and 11.2 MWe of equivalent power correspond to reduced heat losses from the pipelines and fittings. The potential for energy recovery from the pipeline supporting legs is not included in this table.

Table 6. Equivalent power due to heat loss reduction in the CPGF HP and LP pipeline network and net obtainable electric power.

RECOVERABLE ENERGY, MWe						
Case	**Heat losses from pipeline insulation fittings and legs**	**Binary Cycle**	**Biphase Turbine**	**Steam Turbine**	**Turbo - expanders**	**Additional steam**
Heat losses due to fluid transport	**17.6 + 1.46 + 6.17 ***					
Case1: Expansion from 500 to 230 psig			**15.1**	**19.8**	**20.7**	
Case2: Residual energy of separated water		**32.3**				
Case3: Substitution of valves at CP4 inlet				**4.7**	**5.1**	
Case4: Parallel Ducts CP2 & CP3 to CP1				**10.2**	**11.0**	
Case5: Extra layer of insulation	**7.1 + 0.72 + 0.0 ****					
Case6: Third branch in CP2						**2.4**
SUM	**10.5 + 0.72 *****	**32.3**	**15.1**	**34.7**	**36.9**	**2.4**
TOTAL POTENTIAL	**82.82 (71.6+11.22)**					

Notes: *Heat loss from pipelines, fittings and supporting legs; **It is assumed that heat losses from fittings are reduced by 50% when covered with a 2" layer of thermal insulation. Pipeline legs not insulated due to technical and practical reasons; ***Difference of actual heat losses from insulation and fittings and losses using a 1" extra layer of insulation on pipelines and 2" on fittings

5. CONCLUSIONS

1st and second law efficiencies of the separation are low mostly due to the combined effect of deteriorated or absence of thermal insulation and to throttling in the production orifice plate. The corresponding 1st and second law efficiencies of the partial and overall steam transportation processes are also affected by large heat losses caused by the degree of deterioration or absence of the insulating materials of the pipelines and fittings. These losses in turn give rise to a large amount of condensed steam, reduced availability of steam at the power plants and a de-rating of the generating units. Energy losses in the separation process were 1.9% of the produced energy. The corresponding losses in the overall transportation process were 4.7% (180.1 MWt) of the energy carried by the steam after separation. Approximately, 70.2 % (126.6 MWt) of these losses occurred in the HP network and 29.8% (54.3 MWt) in the LP network. Pipelines contributed with 45.7% (57.9 MWt) of the energy losses in the HP network, pipeline fittings with 19.5% (24.7 MWt) and condensate drains with 34.8% (44.0 MWt). The corresponding composition of the heat losses in the LP network were 28.1 % (15.0 MWt), 16.2% (8.6 MWt) and 55.7% (29.8 MWt), respectively. Energy losses during steam transportation are largely caused by the deterioration of the insulating materials of the pipelines and fittings which, in turn, increase steam condensation, and therefore heat losses from the drained fluids increase significantly. 18-20% of the total pipeline network length had insulations with deteriorated to very bad condition (qualities C and D, respectively) and accounted for nearly half of the heat losses, 48% and 43%, for both gathering networks, respectively. It is recommended to provide extensive maintenance of the insulation materials to restore its design condition to reduce steam condensation and power plant de-rating. The potential for energy recovery amounted 82.8 MWe of electrical power in the fluid production and transportation system, which is equivalent to improving energy utilization by 11.5% over the present installed capacity in the field.

Acknowledgements. Thanks are due to the authorities of Comisión Federal de Electricidad and Instituto de Investigaciones Eléctricas, Mexico, for permission and support to publish this work.

6. REFERENCES

Aqui, A.R., Aragones, J.S., and Amistoso, A.E.: Optimization of Palinpinon-1 production field based on exergy analysis – The Southern Negros geothermal Field Philippines, Proceedings, World Geothermal Congress 2005, Antalya, Turkey, (2005), 24-29 April, 7 pp.

Bettagli, N., and Bidini, G.: Larderello-Farinello-Valle Secolo geothermal area: Exergy analysis of the transportation network and of the electric power plants, Geothermics, **25**, (1996), 3-16.

DiMaria, F.: Design and off-design pipe network geothermal power plant analysis with power pipe simulator, *Energy Conversion and Management*, **41**, (2000), 1223-1235.

DiPippo, R.: *Geothermal power plants: principles applications and case studies*, Butterworth-Heinemann, 2nd ed., Boston, (2005), 450 pp.

Garcia-Gutierrez, A., Martinez-Estrella, J.I., Ovando-Castelar, R., Canchola-Felix, I., Mora-Perez, O., and Gutierrez-Espericueta, S.A.: Improved energy utilization in the Cerro Prieto Geothermal Field fluid transportation network, Transactions Geothermal Resources Council, **36**, (2012), 1061-1066.

Garcia-Gutierrez, A., Martinez-Estrella, J.I., Ovando-Castelar, R., Vazquez-Sandoval, A., and Rosales-Lopez, C.: Thermal performance of the Los Humeros geothermal field fluid transportation network, Transactions Geothermal Resources Council, **37,** (2013), 709-713.

Garcia-Gutierrez, A., Martinez-Estrella, J.I., Ovando-Castelar, R., Canchola-Felix, I., and Jacobo-Galvan, V.P.: Energy Recovery in the Cerro Prieto Geothermal Field Fluid Transportation Network, These proceedings, (2015).

Incropera, F.P., DeWitt, D.P. and Bergman, T.L. *Fundamentals of heat and mass transfer*, 6th Edition, Wiley, (2006), 152-153.

Kaplan, U. and Schochet, D.N.: Improving geothermal power plant performance by repowering with bottoming cycles, Proceedings, World Geothermal Congress 2005, Antalya, Turkey, (2005), 24-29 April, 4 pp.

Kwambai, C.B.: Exergy analysis of Olkaria I power plant, Kenia, The United Nations University, Geothermal Training Program, Reports 2005, Number 5, Orkustofnun, Grensasvegur 9, Is-108, Reykjavik, Iceland, (2005), 37 pp.

Marconcini, R. and Neri, G.: Numerical simulation of a steam pipeline network, *Geothermics*, **7**, (1979), 17-27.

Ovando-Castelar, R., Martinez-Estrella, J.I. Garcia-Gutiérrez, A., Canchola Félix, I., Miranda-Herrera, C.A., and Jacobo-Galvan, V.P.: Estimation of the heat losses of the Cerro Prieto geothermal field steam transportation network based on the pipeline thermal insulation condition, Transactions Geothermal Resources Council, **36**, (2012), 1111-1118.

Ozturk, H.K., Talay, A.O., and Yilanci, A.: Energy and exergy analysis of Kizildere geothermal power plant, Turkey, *Energy Sources, Part A*, **28**, (2006.), 1415-1424.

Peña, J.M., Energy losses in horizontal steam lines, Transactions Geothermal Resources Council, **10**, (1986), 347-252.

Peña, J.M., and Campbell, H.: Evaluación de las pérdidas de calor en líneas de vapor geotérmico. Proceedings, 3rd. Latin American Congress on Heat and Mass Transfer, Guanajuato, Gto., (1988), 4-7 July, 53-64.

Quijano, J.: Exergy analysis for the Ahuachapan and Berlin geothermal fields, El Salvador, Proceedings, World Geothermal Congress 2000, Kyushsu-Tohoku, Japan, (2000), May 28-June 10, 861-865.

White, B. and Morris, G.: Wairakei energy and efficiency audit. Technical report prepared for Contact Energy, Ltd., (2000), 19 pp. Available at http://www.nzgeothermal.org.nz/publications/ studies/WairakeiEfficiencyStudy.pdf.